

A straightforward route to obtain zirconium based metal-organic gels

Janire Santos-Lorenzo^{a,†}, Rubén San José-Velado^{a,†}, Jonathan Albo^b, Garikoitz Beobide^a, Pedro Castaño^c, Oscar Castillo^{a,*}, Antonio Luque^a and Sonia Pérez-Yáñez^{a,d,*}

^aDepartamento de Química Inorgánica, Facultad de Ciencia y Tecnología, Universidad del País Vasco/Euskal Herriko Unibertsitatea, UPV/EHU, Apartado 644, E-48080 Bilbao, Spain.

^bDepartamento de Ingenierías Química y Biomolecular, Universidad de Cantabria, E-39005 Santander, Spain.

^cDepartamento de Ingeniería Química, Facultad de Ciencia y Tecnología, Universidad del País Vasco/Euskal Herriko Unibertsitatea, UPV/EHU, Apartado 644, E-48080 Bilbao, Spain.

^dDepartamento de Química Inorgánica, Facultad de Farmacia, Universidad del País Vasco/Euskal Herriko Unibertsitatea, UPV/EHU, E-01006 Vitoria-Gasteiz, Spain.

†These authors contributed equally.

*Corresponding authors. E-mail addresses: oscar.castillo@ehu.eus (O. Castillo),
sonia.perez@ehu.eus (S. Pérez-Yáñez)

Keywords: zirconium, metal-organic gel, CO₂ electroreduction, porosity, green chemistry

ABSTRACT:

Zirconium based metal-organic gels are obtained through a rapid method at room temperature, employing green solvents, in which the role of water is important. These porous materials, decorated with Brønsted acid sites, show outstanding thermal and chemical stability prompting them as stable catalyst in the continuous electroreduction of CO₂.

1. Introduction

Metal-organic frameworks (MOFs) are nowadays one of the most relevant research fields in materials science [1]. These highly ordered crystalline porous materials owe their relevance mainly to their high surface areas, tunable pores and intriguing functionalities. Moreover, when compared to traditional porous solid materials (i.e. zeolites and activated carbons) MOFs have demonstrated to fulfill several applications [2]. However, their industrial applicability is sometimes hampered by their poor shaping and processability together with their usual poor stability [3]. The reversible nature of coordination bonds affords peculiarities to this kind of compounds not achievable for other materials, but can also be regarded as one of the major drawbacks for their industrial application in several areas [4]. In order to surpass the disadvantage of the instability, some years ago Zr-based MOFs appeared as promising materials. Lot of efforts have been devoted to the progress of this type of materials since their outstanding stability, together with the already relevant properties of MOFs, make Zr-based compounds a keystone in the area of porous materials [5]. Once the problem of the poor stability seems to be overcome, materials with the desired shapes are required. As MOFs are generally obtained as microcrystalline powders, a post-synthetic procedure is employed to achieve the aforementioned requisite. In this way, the shaping of the material is performed with the necessity of employing binders or additives which leads to a reduced adsorption capacity of the material [6]. Keeping in mind this aspect, lately, there has emerged a class of materials called MOGs (metal-organic gels) in which shaping drawbacks of MOFs are far exceeded [7]. Therefore, the combination of Zr-based compounds with the suitable gelation process could shed light on the industrial implementation of this type of materials. Up to date a few works dealing with MOGs have been published [8-10], including a work with some archetypical zirconium based MOFs that led to metal-organic gels [11]. However, most of the MOGs previously reported are obtained through an energetically demanding route (i.e. employing heating procedures) and with environmentally unsustainable solvents such as N,N-dimethylformamide, N,N-dimethylacetamide or hydrochloric acid. Moreover, during the last

years the development of nanocomposites via green protocols affords a promising alternative to porous/mesoporous catalyst supports [12-15].

Herein, we explore some zirconium based systems with the aim of offering a simple and rapid method to obtain gels. Conventional drying procedures lead to a notorious shrinkage of the original gel to provide the corresponding xerogel, in which a remarkable decrease of porosity takes place, rendering usually a non-porous material. However, when they are subjected to a supercritical drying process, the resulting aerogels retain their original porous architecture. Due to their morphological and chemical features, these materials have been evaluated as electrodes in the electrocatalytic reduction of CO₂, a challenging issue of our society in concordance with the achievement of a carbon neutral energy cycle [16].

2. Experimental

2.1. Samples

For our purpose, we focused on UiO-66 [17], MOF-801[18] and MOF-808[18] metal-organic frameworks, all of which share the octahedral $[\text{Zr}_6(\mu_3\text{-O})_4(\mu_3\text{-OH})_4]^{12+}$ building unit that is 12-fold connected (through terephthalate and fumarate ligands in UiO-66 and MOF-801, respectively) or 6-fold linked (through trimesate in MOF-808) to adjacent octahedra. The resulting three-dimensional frameworks are well-known for their very high surface area and unprecedented stability [19-20]. Table 1 gathers the sample coding, and formulae of the gels herein obtained upon the optimum conditions, while the synthesis procedure for each sample is described in the Supplementary data.

Table 1

3. Results and discussion

In a general procedure, ZrCl₄ is dissolved in a mixture of solvent/H₂O. Afterwards, the metal source is added to the solution containing the carboxylic ligand. Then, the resulting solution is

left unaltered, and the outcome is inspected by means of tube inversion test to determine whether the gel is formed or not. As each metal-organic system requires its own gelation conditions, in order to set the optimum parameters, we scrutinized several synthetic parameters such as solvent, metal salt, reagent ratio, addition order, concentration, and temperature (see S1 and S2 sections in the Supplementary data). Solvent, water ratio and addition order were found to be the most crucial aspects. Precisely, only methanol and DMF provided stiff gels, but as long as the water is within a specific ratio range. For instance, in Zr-MOG-1 when H₂O:Zr ratio is comprised between 3.4 and 13.4, the gel is formed in 1-2 minutes (Fig. 1a). Somewhat higher H₂O:Zr ratios (up to 35) lengthen monotonically the gel formation time (40 minutes). Out of these limits the time required by the gelation subtly increases.

It must be noted that the formation of the coordination polymer nodes (i.e. polyoxometalate type cluster) requires water in the reaction media. So that, the addition of a quasi-stoichiometric amount of water provides oxide and hydroxide bridges required for the formation of the cluster, without being so high as to promote further polymerization into more extended insoluble polymeric species. Then, the addition of the polycarboxylic acid promotes the polymerization reaction by cross-linking the zirconium nodes. The lowering of the pH by addition of HCl impedes the gelation, since it hinders the deprotonation and coordination of the ligand. On the contrary, the addition of base boosts the reaction too much and particulate gels are obtained (Fig. 1b). With regard to the influence of the addition order, if Zr(IV) source and the polycarboxylic acid are mixed prior to the addition of water, the direct coordination of the carboxylic ligand to the Zr(IV) centers saturates its coordination sphere precluding the inclusion of oxides and hydroxide anions in a later stage.

Figure 1

To get deeper insight into the role of water we carried out ESI-MS (electrospray ionization-mass spectrometry) measurements on the reagent mixture prior to the addition of the carboxylic

acid (see S3 section of the Supplementary data). ESI-Mass spectroscopy studies performed over a 0.332 M $ZrCl_4$ methanolic solution adding a small amount of water (v/v: 2%) and without adding it, indicate that significant changes take place (Fig. 2, Fig. S.2 and Fig. S.3). In the methanol solution, halozirconates and mixed zirconium methoxide/chlorides are predominant, while when adding water mainly water-coordinated species are observed and the Zr:Cl ratio is highly reduced. It is also worth mentioning that upon the addition of water a bunch of signals appears with a 0.5 periodicity (indicative of a -2 charge) at m/z values around 500-575, probably due to the presence of polynuclear species based on oxide and hydroxide bridges. Upon the addition of the carboxylic acid, the aforementioned zirconium complexes evolve to $[Zr_6(\mu_3-O)_4(\mu_3-OH)_4]^{12+}$ type cluster as corroborated by the FTIR and XPS spectra of the final products (see S4 and S5 sections of the Supplementary data). The shape and position of the zirconium 3d peaks ($3d_{3/2}$ and $3d_{5/2}$) resemble the data available in the literature for related MOFs (MOF-808, UiO-66 and MOF-801) [21-23], featured all of them by the hexanuclear Zr cluster.

Figure 2

With the aim of providing deeper insight into the nature of the metal-organic gels, we performed powder X-ray diffraction (PXRD) measurements upon the samples, in order to tie together Zr-MOG-1, Zr-MOG-2 and Zr-MOG-3 with their related MOFs (MOF-808, UiO-66 and MOF-801, respectively). In this sense, PXRD patterns of the samples (Fig. S.9) revealed a broad signal between $2\theta = 6-10^\circ$ ($d = 14.7-8.8 \text{ \AA}$) which indicates a kind of ordering which can be related to the contribution of the most intense reflections of each of the corresponding related MOFs within the measured 2θ range. For instance, the diffraction patterns for UiO-66 show peaks at $2\theta 7.4^\circ$ ($d = 11.9 \text{ \AA}$) and 8.6° ($d = 10.2 \text{ \AA}$) corresponding to (111) and (200) reflections, respectively, while in the isorecticular MOF-801 these reflections appear at $2\theta 8.6^\circ$ ($d = 10.2 \text{ \AA}$) and 9.9° ($d = 8.9 \text{ \AA}$) [17-18]. The main reflections for MOF-808, (220) and (311), emerge at 2θ

7.1° ($d = 12.4 \text{ \AA}$) and 8.4° ($d = 10.5 \text{ \AA}$), respectively [18]. All these reflections can be related to the interplanar distances between zirconium cluster arrays set by the bridging ligand. In this regard, the terephthalate ligand imposes the greatest cluster···cluster distance (UiO-66: 14.7 \AA), and therefore, it sets the greatest interplanar distances between cluster arrays. Accordingly, its diffraction maximum appears at lower 2θ values in comparison with those implying shorter bridging distances (Zr-MOG-3: 12.6 \AA and Zr-MOG-1: 12.4 \AA). Several post-synthetic solvothermal treatments were performed with the aim of improving the crystallinity of the material, although none of them worked.

Supercritical drying of the gels led to highly porous translucent monoliths which microstructural features were studied by N_2 physisorption at 77 K and scanning electron microscopy (SEM). The N_2 isotherms of the aerogels feature an IUPAC type II isotherm characteristic of macroporous materials with a mesoporous contribution as indicated by the hysteretic desorption isotherm (Fig. S.12) [24]. Subtracted porosity data is gathered in Table S.5. The compounds show moderate specific surface areas (219 , 377 and $52 \text{ m}^2 \text{ g}^{-1}$, for Zr-MOG-1, -2 and -3, respectively). The total pore volumes follow the same trend (1.14 , 5.00 and $0.32 \text{ cm}^3 \text{ g}^{-1}$, respectively) and, interestingly, the values of Zr-MOG-1 and -2 are relatively high when compared to MOFs holding the highest pore volumes (1.14 – $4.40 \text{ cm}^3 \text{ g}^{-1}$) [25]. Note that the porosity of these MOGs is mainly attributed to their microstructural features which is in concordance with the aforementioned lack of crystallinity of the coordination polymers and the small size of the particles (15 – 30 nm) that constitute the porous monoliths observed in SEM images (Fig. 3 and Fig. S.11).



Figure 3

According to the thermogravimetric data, all samples show an initial mass loss corresponding to physisorbed solvent and humidity, after which the coordination framework of Zr-MOG-1 and Zr-MOG-2 remains stable up to *ca.* $400 \text{ }^\circ\text{C}$ (Fig. S.6 and Fig. S.7). This value is

in concordance with the foreseen thermal stability of zirconium-based MOFs [5,26]. The earlier decomposition of Zr-MOG-3 (*ca.* 320 °C) is related to the lower stability of the non-aromatic fumarate ligand (Fig. S.8). In addition to their thermal stability, the chemical stability of the metal-organic gels was evaluated (see section S10 of the Supplementary data). The gels were subjected to chemical inertness tests based on the immersion of a slice of gel for 24 h in a series of the most usual chemical scenes. Accordingly, Zr-MOGs remain stable upon the exposure to common organic solvents such as acetonitrile, chloroform and N,N-dimethylformamide, as well as to aqueous solution of different acidity. Zr-MOG-1 was the chemically most resistant gel, remaining unshakeable in a wide range of pH values (from 1 to 12), and even in concentrated HNO₃ (69%). Only very basic conditions were able to break the gels up which is in concordance with the previously described behaviour of Zr-MOFs in alkaline media [5]. Furthermore, inspired by the stiffness of previously reported gels and aerogels, we accomplished uniaxial quasistatic compression tests upon herein prepared aerogels (Figure S.18). In this case, the compression-strain curves indicate that these aerogels behave as brittle materials holding relatively low strain values (stress: $2.3 \cdot 10^{-2}$ – $5.8 \cdot 10^{-2}$ MPa; strain: below 20%) comparable to other metal-organic aerogels.[8] No correlation has been found between the mechanical behaviour and the thermogravimetric results.

Zirconium MOFs are known by exhibiting different types of Brønsted acid sites [27]. Thus, to determine if the herein reported metal-organic gels present comparable surface acidity we performed an acid-base titration upon Zr-MOG-1. This analysis revealed four types of protons in Zr-MOG-1 with the following pK_a values: 3.3, 5.1, 6.7 and 7.7. In a previous study [28], Farha and coworkers pointed out the existence of three pK_a values attributable to bridging μ₃-OH (pK_a = 3.6) and to terminal –OH₂ (pK_a = 6.2) and –OH (pK_a = 8.2) groups that replace missing linkers in zirconium cluster. In our case, the additional pK_a value (5.1) can be related to the presence of protonated –COOH groups as referred in the formula (see Table 1). In fact, it fits rather well the pK_{a3} (4.7) of trimesic acid [29]. Note that the nanometric size of the particles renders a faulty external surface furnished by defect sites resulting from either a surfeit or

shortage of linkers around the clusters which accounts for the surface acidity. The same studies were performed for the remaining MOGs (see ESI).

To get further knowledge on the potential applicability of these materials we decided to analyze the performance of Zr-MOG-1 as catalyst in the continuous electroreduction of CO₂ into valuable chemicals which is nowadays one of the challenges for sustainable development [30-31]. Although metal and metal oxides have been widely studied as electrocatalyst in CO₂ reduction, recently a series of MOFs and MOGs have demonstrated their activity rendering reduction products such as oxalic acid, formic acid, methanol and ethanol [32-34]. In this regard, apart from the activity expected for the zirconium sites of Zr-MOG-1, the presence of Brønsted acid sites in the surface of the materials can provide a proton source in the formation of reduction products. The results revealed the formation of formic acid as single product in the liquid fraction which is a valuable chemical that can be used in a variety of traditional industrial uses including pharmaceutical synthesis, pulp production or textile industry [35]. Measured production rates and efficiencies (24.4-43.1 $\mu\text{mol m}^{-2} \text{s}^{-1}$ and 2.3–4.2 %, respectively; see section S13 of the Supplementary data) were comparable to those provided by other MOFs but are below the ones corresponding to best performing inorganic materials. In spite of it, a striking feature is that the material remains stable after 7 h of operation, which denotes no leaching or degradation of the material. This behaviour makes this material appealing for the long term runs required in real application.

4. Conclusions

All in all, only under well-selected synthetic conditions the gelation succeeded, being remarkable the role that water plays in the formation of cluster seeds, after which a sudden and massive nucleation process occurs upon the addition of polycarboxylic ligand, leading to well set up metal-organic gels. These conditions have allowed us to form zirconium metal-organic gels in a rapid manner (1-2 minutes) without employing modulators such as HCl and acetic acid. As a result, the reported gelation process endows Zr-based amorphous materials exhibiting a porous microstructure with an outstanding thermal and chemical stability. These materials are

based on $[\text{Zr}_6(\text{OH})_4(\text{O})_4]^{12+}$ clusters as corroborated from PXRD, XPS and FTIR analysis. The inner surface of the metal-organic gels is decorated with non-deprotonated carboxylic groups. Additionally, the $[\text{Zr}_6(\text{OH})_4(\text{O})_4]^{12+}$ cluster also presents acid protons due to the hard acid nature of the zirconium(IV) cation. All these features make the materials suitable for a branch of industrial applications, among which catalysis is a very promising one as it depends on the local structure of the active sites regardless of the presence or not of long range ordering. In this sense, the herein reported MOGs have been tested as electrodes in the electrocatalytic reduction of CO_2 , showing a promising performance towards the generation of formic acid.

Acknowledgments

This research has been funded by Ministerio de Economía y Competitividad (MAT2016–75883–C2–1–P) and Universidad del País Vasco/Euskal Herriko Unibertsitatea (PPG17/37). J. Albo acknowledges the Ramón y Cajal programme (RYC-2015-17080). The authors thank for technical and human support provided by SGIKER of UPV/EHU and European funding (ERDF and ESF)

References

- [1] H. Furukawa, K. E. Cordova, M. O’Keeffe, O. M. Yaghi, *Science* 341 (2013) 974–985.
- [2] H.-C. Zhou, S. Kitagawa, *Chem. Soc. Rev.* 43 (2014) 5415–5418.
- [3] Y. Chen, X. Huan, S. Zhang, S. Li, S. Cao, X. Pei, J. Zhou, X. Feng, B. Wang, *J. Am. Chem. Soc.* 138 (2016) 10810–10813.
- [4] S. Keskin, T. M. van Heest, D. S. Sholl, *ChemSusChem* 3 (2010) 879–891.
- [5] Y. Bai, Y. Dou, L.-H. Xie, W. Rutledge, J.-R. Li, H.-C. Zhou, *Chem. Soc. Rev.* 45 (2016) 2327–2367.

- [6] D. Bazer-Bachi, L. Assié, V. Lecocq, B. Harbuzaru, V. Falk, *Powder Technol.* 255 (2014) 52–59.
- [7] J. Zhang, C.-Y. Su, *Coord. Chem. Rev.* 257 (2013) 1373–1408.
- [8] D. Vallejo-Sánchez, P. Amo-Ochoa, G. Beobide, O. Castillo, M. Fröba, F. Hoffmann, A. Luque, P. Ocón, S. Pérez-Yáñez, *Adv. Funct. Mater.* 27 (2017) 1605448.
- [9] A. Y.-Y. Tam, V. W.-W. Yam, *Chem. Soc. Rev.* 42 (2013) 1540-1567.
- [10] M. R. Lohe, M. Rose, S. Kaskel, *Chem. Commun.* 0 (2009) 6056–6058.
- [11] B. Bueken, N. Van Velthoven, T. Willhammar, T. Stassin, I. Stassen, D. A. Keen, G. V. Baron, J. F. M. Denayer, R. Ameloot, S. Bals, D. De Vos, T. D. Bennett, *Chem. Sci.* 8 (2017) 3939–3948.
- [12] A. Maleki, Z. Hajizadeh, R. Firouzi-Haji, *Microporous Mesoporous Mater.* 259 (2018) 46–53.
- [13] A. Maleki, Z. Hajizadeh, V. Sharifi, Z. Emdadi, *J. Clean. Prod.* 215 (2019) 1233–1245.
- [14] A. Maleki, *Tetrahedron* 68 (2012) 7827–7833.
- [15] A. Maleki, V. Eskandarpour, J. Rahimi, N. Hamidi, *Carbohydr. Polym.* 208 (2019) 251–260.
- [16] A. Schoedel, Z. Ji, O. M. Yaghi, *Nature Energy* 1 (2016) 16034.
- [17] J. H. Cavka, S. Jakobsen, U. Olsbye, N. Guilluos, C. Lamberti, S. Bordiga, K. P. Lillerud, *J. Am. Chem. Soc.* 130 (2008) 13850–13851.
- [18] H. Furukawa, F. Gándara, Y.-B. Zhang, J. Jiang, W. L. Queen, M. R. Hudson, O. M. Yaghi, *J. Am. Chem. Soc.* 136 (2014) 4369–4381.
- [19] J. B. DeCoste, G. W. Peterson, H. Jasuja, T. Grant Glover, Y.-G. Huang, K. S. Walton, *J. Mat. Chem. A.* 1 (2013) 5642–5650.
- [20] A. U. Czaja, N. Trukhan, U. Müller, *Chem. Soc. Rev.* 38 (2009) 1284–1293.

- [21] G. Wang, C. Sharp, A. M. Plonka, Q. Wang, A. I. Frenkel, W. Guo, C. Hill, C. Smith, J. Kollar, D. Troya, J. R. Morris, *J. Phys. Chem. C* 121 (2017) 11261–11272.
- [22] J. Long, S. Wang, Z. Ding, S. Wang, Y. Zhou, L. Huang, X. Wang, *Chem. Commun.* 48 (2012) 11656–11658.
- [23] F. Ke, C. Peng, T. Zhang, M. Zhang, C. Zhou, H. Cai, J. Zhu, X. Wan, *Scientific Reports* 8 (2018) 939.
- [24] M. Thommes, K. Kaneko, A. V. Neimark, J. P. Olivier, F. Rodriguez-Reinoso, J. Rouquerol, K. S. W. Sing, *Pure Appl. Chem.* 87 (2015) 1051–1069.
- [25] O. K. Farha, I. Eryazicit, N. C. Jeong, B. G. Hauser, C. E. Wilmer, A. A. Sarjeant, R. Q. Snurr, S. T. Nguyen, A. O. Yazaydin, J. T. Hupp, *J. Am. Chem. Soc.* 134 (2012) 15016–15021.
- [26] M. Kandiah, M. H. Nilsen, S. Usseglio, S. Jakobsen, U. Olsbyet, M. Tilset, C. Larabi, E. A. Quadrelli, F. Bonino, K. P. Lillerud, *Chem. Mater.* 22 (2010) 6632–6640.
- [27] Y. Wang, L. Li, P. Dai, L. Yan, L. Cao, X. Gu, X. Zhao, *J. Mat. Chem. A* 5 (2017) 22372–22379.
- [28] R. C. Klet, Y. Liu, T. C. Wang, J. T. Hupp, O. M. Farha, *J. Mat. Chem. A* 4 (2016) 1479–1485.
- [29] E. Serjeant and B. Dempsey, *Ionisation constants of organic acids in aqueous solution*, 1st ed. Pergamon Press, Oxford, 1979
- [30] M. B. Solomon, T. L. Church, D. M. D'Alessandro, *CrystEngComm* 19 (2017) 4049–4065.
- [31] J. Albo, M. Alvarez-Guerra, P. Castaño, A. Irabien, *Green Chem.* 17 (2015) 2304–2324.
- [32] A. Doménech, H. García, M. T. Doménech-Carbó, F. Llabrés-i-Xamena, *J. Phys. Chem. C* 111 (2007) 13701–13711.
- [33] J. Albo, D. Vallejo, G. Beobide, O. Castillo, P. Castaño, A. Irabien, *ChemSusChem* 10 (2017) 1100–1109.

- [34] M. Perfecto-Irigaray, J. Albo, G. Beobide, O. Castillo, A. Irabien, S. Pérez-Yáñez, RSC Adv. 8 (2018) 21092–21099.
- [35] I. C. Um, Y. H. Park, Fibers Polym. 8 (2007) 579–585.

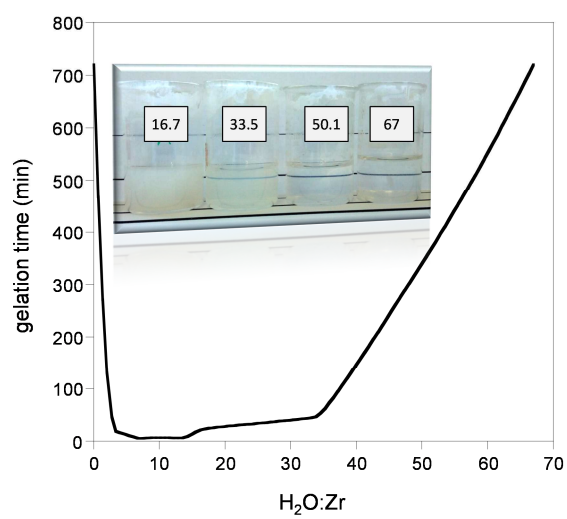
ACCEPTED MANUSCRIPT

Table 1

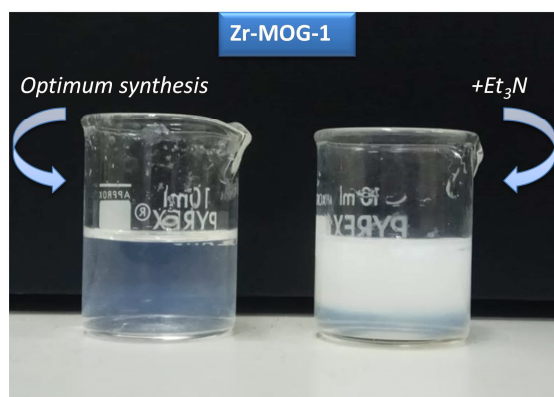
Coding and formulae of prepared metal-organic gels.

Code	Related MOF	Carboxylic ligand	Formula ^a
Zr-MOG-1	MOF-808	Trimesate	$Zr_6O_4(OH)_4(BTC)_{2.13}(HBTC)_{2.81} \cdot n\text{Solvent}$
Zr-MOG-2	UiO-66	Terephthalate	$Zr_6O_4(OH)_4(BDC)_{5.38}(HBDC)_{1.25} \cdot n\text{Solvent}$
Zr-MOG-3	MOF-801	Fumarate	$Zr_6O_4(OH)_4(FUM)_{5.52}(HFUM)_{0.96} \cdot n\text{Solvent}$

^a BTC: benzene-1,3,5-tricarboxylate (trimesate), BDC: benzene-1,4-dicarboxylate (terephthalate), FUM: *trans*-1,2-ethylenedicarboxylate (fumarate).



(a)



(b)

Fig. 1. (a) Gelation time vs H₂O:Zr molar ratio; (b) gels formed upon the lack of base (left) and on its presence (right).

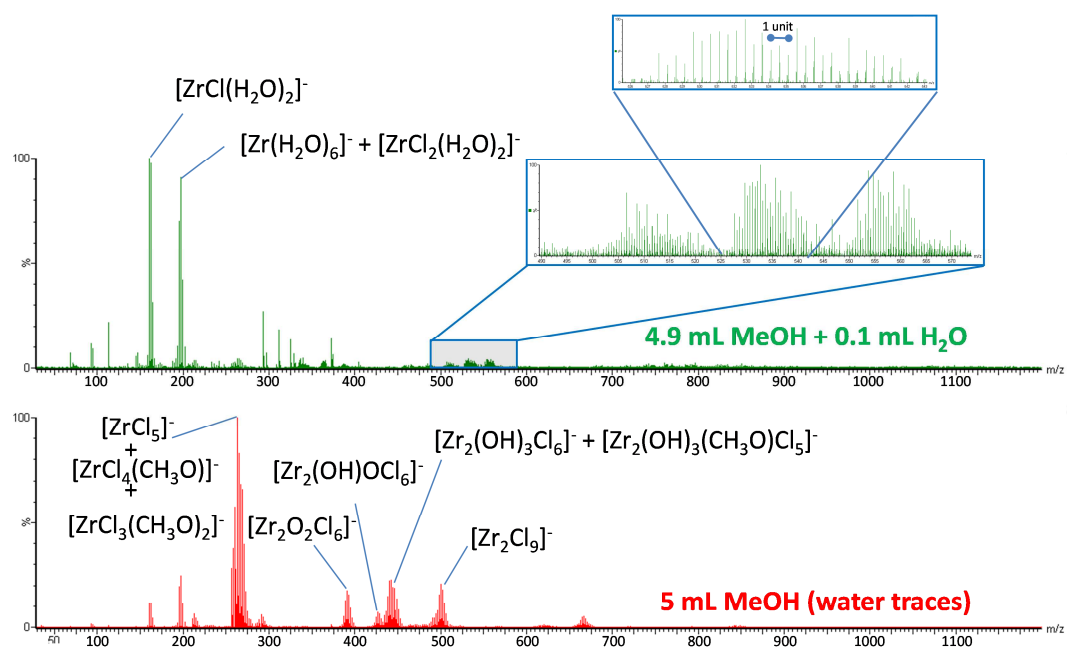


Fig. 2. ESI-Mass spectra of the initial stage during the synthesis procedure in a methanol-water mixture (upper side) and without the addition of water (lower side). The inset in the upper side shows a magnification of $m/z = 490\text{-}580$ range.

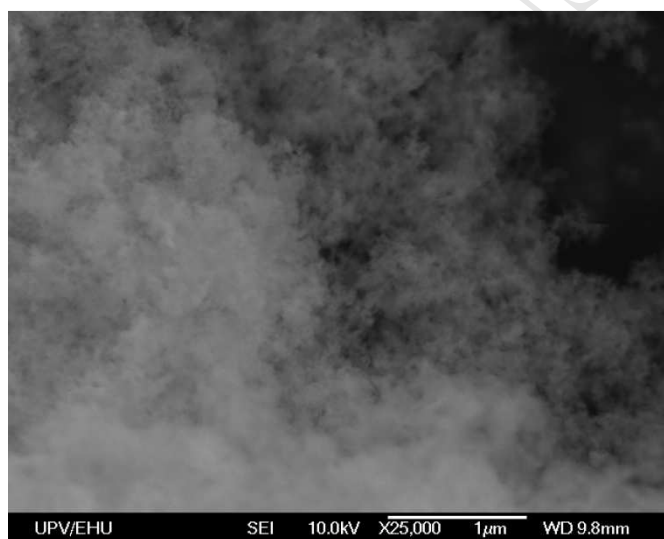
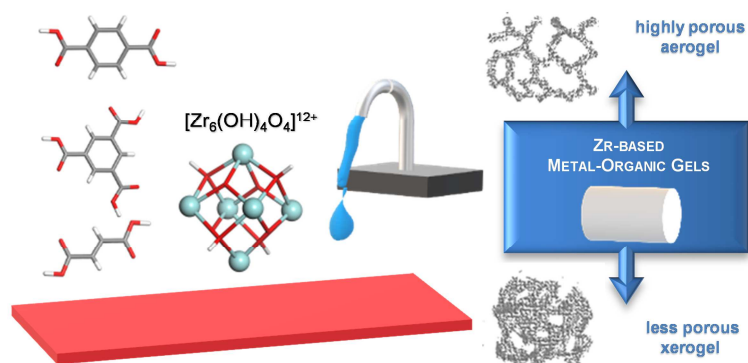


Fig. 3. SEM micrograph of the aerogel corresponding to Zr-MOG-1 at 25 kX magnification.

GRAPHICAL ABSTRACTS

Zirconium based metal-organic gels are obtained through a green and rapid method at room temperature in which the role of water seems to be crucial.



HIGHLIGHTS

- Green and rapid method for achieving zirconium based metal-organic gels (MOGs) at room temperature.
- Porous structure with thermal and chemical stability together with Brønsted acid sites.
- Zr-MOGs as electrodes in the electrocatalytic reduction of CO₂ to formic acid.